

The Thermal Conductivity of Polymer-Derived Amorphous Si–O–C Compounds and Nano-Composites

Aleksander Gurlo,^{‡,¶} Emanuel Ionescu,[‡] Ralf Riedel,[‡] and David R. Clarke^{§,†}

[‡]Fachbereich Material und Geowissenschaften, Technische Universität Darmstadt, Darmstadt, Germany

[§]John A. Paulson School of Engineering and Applied Sciences, Harvard University, Cambridge, Massachusetts 02138

Silicon oxycarbide glasses can be produced over a range of Si–O–C compositions by the controlled pyrolysis of polymer precursors. We present measurements of the thermal conductivity of a silicon oxycarbide glass after two different heat treatments and two Si–O–C nano-composites, hot-pressed at 1600°C, up to 1000°C and compare them to fused silica, amorphous carbon, and SiC. The temperature dependence of their thermal conductivities is similar to other amorphous materials. The presence of low volume fractions of nanoparticles of hafnia (4.5 v/o) or zirconia (7.4 v/o) dispersed within the amorphous matrix only modifies the conductivity slightly, consistent with a simple Maxwell model, and does not affect the temperature dependence of the thermal conductivity above room temperature.

I. Introduction

AMORPHOUS solids consisting of just silicon, oxygen, and carbon can be formed as bulk materials^{1,2} and films.³ As with traditional silicate and germanate glasses, these new glasses can form over a relatively wide compositional range but, in contrast to traditional glasses, they cannot be formed by simply melting or directly from the vapor or sintering and reacting the oxides and carbides. Intriguingly, they can only be formed by the controlled pyrolysis of poly(organo)siloxane precursor compounds, a process that preserves the Si–O–C covalent bonding in the precursor polymer.² These glasses have remarkable high-temperature properties. They are resistant to crystallization to temperatures in excess of 1300°C,¹ are creep resistant and ceramics made from them have demonstrated exceptional resistance to high-temperature oxidation.² These attractive high-temperature properties combined with their low thermal expansion make them candidate materials for thermal protection applications, such as environmental barrier coatings on SiC materials. Some of the silicon oxycarbide glasses can also be heat-treated at very high temperatures (1600°C and above) to form nanocrystalline SiC and turbostratic carbon in a silica matrix² as the carbothermal reduction occurs. At still higher temperatures, typically 1700°C and above, internal carbothermal reduction goes to completion resulting in mass loss and the formation of amorphous silica and the crystallization of β -SiC following a phase separation process.² Furthermore, it has also been demonstrated that nano-composites with an amorphous silicon oxycarbide matrix can be created, either by controlled

crystallization of zirconia and hafnia-doped silicon oxycarbide glass⁴ or by physical mixing of a second Zr- or Hf-containing precursor phase with the precursor polymer prior to pyrolysis.⁵

In this work, we report on the thermal conductivity of one of these amorphous materials compositions, some heat-treated to maximum temperatures of 1100°C and others to 1600°C. Based on the reported microscopy observations of this class of material,^{2,6} it might be expected that the thermal conductivity would be exceptionally low since each of them can be characterized by an amorphous, covalent matrix containing a low volume fraction of nano-scale inhomogeneities or second phases. Furthermore, because of their similarity with other amorphous solids and quantified by the phonon-glass models of Kittel,⁷ Slack⁸ and Cahill and Pohl,⁹ the thermal conductivities can be expected to be similar to that of silica glasses. This is borne out by the results presented here.

II. Experimental Details

The silicon oxycarbide materials studied are listed in Table I. They were prepared from a commercial poly(methylsilsesquioxane) starting polymer (Wacker-BelsilTM PMS MK[®], Wacker Chemie AG, Burghausen, Germany) together with zirconium acetylacetonate as a cross-linking agent. A batch of the polymer was cross-linked at 250°C for 30 min (chamber furnace, N30/659HA; Nabertherm GmbH, Lilienthal, Germany), ball-milled and then sieved to a particle size <100 μ m to produce coarse, cross-linked particles. These were then pyrolyzed in flowing argon up to the temperature of 800°C for 30 min (alumina tube furnace, HTSS 100-500; Carbolite Geo, Neuhausen, Germany) and then mixed in a ratio of 3:1 with catalytically treated and cross-linked polymer (75 wt% MKF + 25 wt% MK polymer) by ball-milling and finally sieved to a particle size <100 μ m. These polymer powders were used as the starting powders for subsequent processing.

One batch of powders was warm pressed into cylindrical pellets in a metallic die at 25 MPa and 18 °C. (machine type 123, H. Collin) before given a final pyrolysis treatment at 1100°C for 5 h in an argon atmosphere. The second batch of powders was pyrolyzed at 900°C in argon for 2 h, ball-milled and sieved, and then compacted at 1600°C for 30 min under a pressure of 30 MPa. The Si–O–C-zirconia nano-composites were made in the same way except that the polysilsesquioxane precursor was first chemically modified with $Zr(O^iPr)_4$ in argon at –80°C and then subsequently pyrolyzed at 900°C in argon before finally hot-pressing at 1600°C. The Si–O–C hafnia nano-composite was prepared identically but modified with $Hf(O^iPr)_4$ rather than with $Zr(O^iPr)_4$. The nano-composite materials were prepared as part of a detailed study of their high-temperature properties.

After fabrication, all the materials were black in color, presumably due to optical absorption associated with the excess carbon they contained. Their chemical composition

D. J. Green—contributing editor

Manuscript No. 37395. Received August 23, 2015; approved August 25, 2015.

[¶]Present address: Fachgebiet Keramische Werkstoffe, Institut für Werkstoffwissenschaften und -Technologien, Technische Universität Berlin, Hardenbergstraße 40, D-10623 Berlin, Germany

[†]Author to whom correspondence should be addressed. e-mail: clarke@seas.harvard.edu

Table I. Compositions Studied

Composition	Densification method	SiO ₂ (vol%)	SiC (vol%)	“Free” carbon (vol%)	Open porosity (vol%)	Second phase (vol%)
SiO _{1.59} C _{0.66}	Hot-pressed @ 1600°C	77.5	9.11	13.35	0	—
SiO _{1.82} C _{0.42} Zr _{0.1}	Hot-pressed @ 1600°C	77.63	8.46	6.55	0	7.36
SiO _{1.77} C _{0.42} Hf _{0.06}	Hot-pressed @ 1600°C	80.46	7.79	7.22	0	4.52
SiO _{1.54} C _{0.53}	Sintered @ 1100°C	72.0	9.11	6.2	12	—

was determined by coupled plasma atomic emission spectroscopy (iCAP 6500; Thermo Sciences Instruments, Waltham, MA) and the element analyzer (Pascher) at Mikro-Labor Pascher (Remagen, Germany). Raman spectroscopy was carried out using a LabRam Horiba Raman system with 532 nm laser excitation.

The thermal conductivity, κ , of the samples was calculated from measurements of the thermal diffusivity, density, and both measurements and calculations of the heat capacity using the standard relationship:

$$\kappa = \rho C_v \alpha \quad (1)$$

where ρ is the density, C_v the heat capacity, and α the thermal diffusivity. The thermal diffusivities were measured using a standard laser flash method (Netzsch LFA 457 instrument, Netzsch Instruments North America, Burlington, MA) in a flowing argon atmosphere up to 1000°C. Before the measurements, the samples were first coated with a thin layer of gold and an adhesion layer of titanium to block radiative transport of the laser flash through the samples and then a thin colloidal layer of graphite to maximize absorption and emissivity. Measurements were repeated three times, and made on both heating and cooling. Diffusivities were also measured down to 153 K for the hot-pressed SiO_{1.59}C_{0.66} material. Density measurements of the samples were made by the Archimedes method. Heat capacity measurements were made using differential scanning calorimetry from room temperature to ~300°C. These were extended to higher temperatures using the Neumann–Kopp rule. The intrinsic thermal conductivity of the materials (κ_{int}) were calculated after taking into account the effect of the presence of small volume fraction (ϕ) of porosity, determined from density measurements, through the usual Maxwell relation for the measured conductivity (κ_{meas})^{10,11}

$$\kappa_{\text{int}} = \kappa_{\text{meas}} \left(1 - \frac{3\phi}{2} \right) \quad (2)$$

The microstructures of the materials studied in this work have previously been studied by transmission electron microscopy,^{4,12} Raman and X-ray diffraction. Both HRTEM and X-ray diffraction of the SiO_{1.54}C_{0.53} material, sintered to 1100°C indicates that they are noncrystalline containing clusters of nano-sized pores and SiC on the internal surfaces of the pores.² The SiO_{1.59}C_{0.66} materials hot-pressed at 1600°C, were noncrystalline, a finding substantially confirmed by HRTEM but TEM also indicates a small volume fraction of very small (1–2 nm) crystallites of SiC as well as small regions of high-aspect turbostratic carbon. This is consistent with previous NMR results¹³ which also suggest that the noncrystalline phase is predominately SiO₂ with few SiO_xC_{4-x} mixed bonded tetrahedra. The hot-pressed nanocomposites had the same amorphous matrix microstructure with dispersed nanoparticles of zirconia or hafnia.¹²

III. Results

The thermal conductivities as a function of temperature are shown in Fig. 1 for the Si–O–C compounds and in Fig. 2 for

the nano-composite materials. Also shown in Fig. 1 for comparison are literature values for fused silica, an amorphous carbon¹⁴ as well as the reported conductivity perpendicular to the graphitic sheets in graphite references.^{15,16} As shown in Fig. 1, the thermal conductivity of the material prepared at 1100°C has a similar temperature dependence as the fused silica but is significantly lower. It is also significantly lower than that of the other materials shown in Fig. 1. The values shown were computed using an estimate of porosity from the density measurements but as there is some uncertainty as to the theoretical physical density of the Si–O–C network the estimate may be slightly in error. The conductivity of the hot-pressed SiO_{1.59}C_{0.66} composition has an almost identical thermal conductivity from 153 K (the lower limit of our measurement capabilities) to 500°C as fused silica. (As will be discussed later, although having a similar conductivity might be expected, having almost exactly the same conductivity is probably a coincidence). Although we have not made measurements down to cryogenic temperatures, the thermal conductivity down to 153 K clearly superimposes on that of fused silica. At the upper temperatures, fused silica exhibits a slight upturn, which may be due to radiative transport, whereas this is not found with the SiO_{1.59}C_{0.66} material for temperatures up to 1273 K. As the mean molar mass of a pure Si–O–C glass (i.e., free of excess, segregated carbon) is expected to be lower than that of fused silica, one might anticipate that the conductivity of the pure Si–O–C glass will be somewhat higher than that of fused silica.

The thermal conductivities of the nano composites are similar to those of the hot-pressed Si–O–C matrix material, differing only in their numerical values. This finding is consistent with the expectation from the microstructural studies

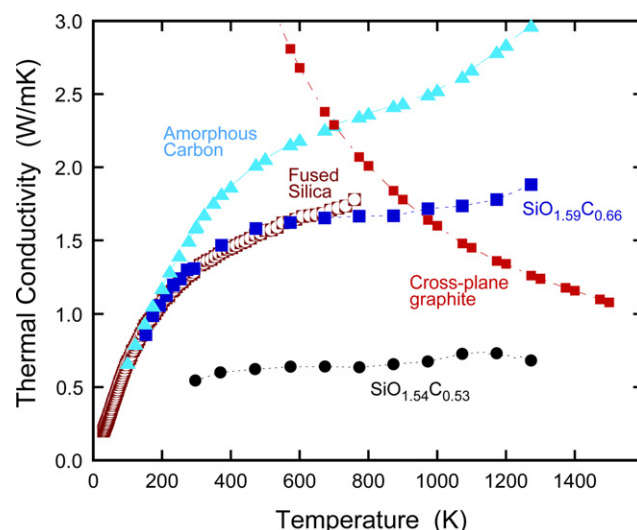


Fig. 1. A comparison of the thermal conductivities of two amorphous silicon oxycarbides, SiO_{1.59}C_{0.66} and SiO_{1.54}C_{0.53}, with fused silica,²⁵ graphite, and with amorphous carbon.²⁶ The thermal conductivity of neutron-amorphous SiC is reported to be significantly higher, ~4 W·(m·K)⁻¹,²³ and so is not shown. The two amorphous silicon oxycarbides were synthesized in the same way up to 1100°C but the SiO_{1.59}C_{0.66} material was subsequently hot-pressed in argon to 1600°C. The measurement uncertainty for the silicon oxycarbide data is approximately the same as the symbol size.

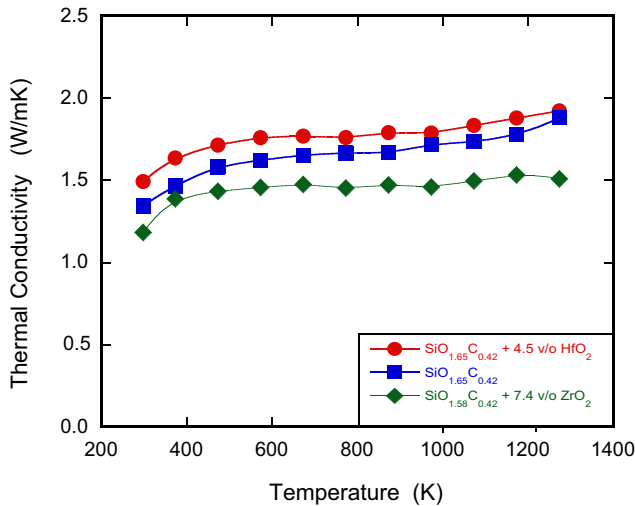


Fig. 2. The thermal conductivity of three nano-composites containing dispersed nanoparticles of either zirconia or hafnia, as indicated in the figure legend. For comparison, the thermal conductivity of the matrix material, $\text{SiO}_{1.65}\text{C}_{0.42}$, is shown. All the materials, hot-pressed at 1600°C , have the characteristic temperature dependence of amorphous solids, rising with temperature around room temperature and then almost independent of temperature thereafter. Again, the measurement uncertainty is approximately the same as the symbol size.

showing dispersed particles in a continuous Si–O–C matrix.¹² As can be seen from Fig. 2, there is a small difference between the hot-pressed matrix material and those containing hafnia and zirconia nano-particles. The lower conductivity material, containing amorphous zirconia particles, also has a higher carbon content than the other nano-composites.

The Raman spectra of all the materials studied were similar, consisting of a broad line at $\sim 1357\text{ cm}^{-1}$ (sometimes referred to as the D line in studies of carbon polymorphs^{17,18}) and a weaker overlapping doublet centered at ~ 1600 and $\sim 1626\text{ cm}^{-1}$, the latter due to disorder (Fig 3). The position of this doublet coincides with the spectral position of the G line, present in graphite and graphene, which is associated with sp^2 bonding. Unlike in graphite or graphene, however, the intensity of the lines at 1357 cm^{-1} is higher than that of the lines at 1600 cm^{-1} . (Highly crystalline graphite does not exhibit the D band but it appears in poorly crystalline graphite as a result of disorder and the presence of defects). In addition, the materials showed a weak doublet at 2700 cm^{-1} , which are characteristic of the second-order Raman D lines of the amorphous carbon. No doublet at 2700 cm^{-1} was detectable in the material densified at 1100°C , but this may be attributed to the weaker Raman signal from this material. It is notable that the spectra from the nano-composites are essentially indistinguishable from the silicon oxycarbide matrix material suggesting that the presence of the nanoparticles has not affected the structure of the carbonaceous material. It was not possible to make quantitative comparisons of the Raman intensities between the materials but the intensity of both the G and D bands, relative to the background, increased with the processing temperature. Based on the analysis of the width of the Raman lines following the procedure presented by Ferrari and Robertson,¹⁸ the size of the carbon crystallites in each of the materials is estimated to be 1.5–2.0 nm.

IV. Discussion

The most striking features of the data in Figs. 1 and 2, are that the thermal conductivities of the polymer-derived amorphous Si–O–C materials all have rather similar values and they also exhibit a temperature dependence characteristic of amorphous solids being almost independent of temperature

above room temperature.⁹ Based on the prior characterizations⁴ of the microstructures of these materials by transmission electron microscopy and X-ray diffraction, the conductivity data can be understood as being due to a continuous, low thermal conductivity amorphous phase containing a minor volume fraction of one or more second phases dispersed within it. For the materials prepared at temperatures up to 1400°C and illustrated by the data of the 1100°C material, the continuous phase is an amorphous Si–O–C matrix containing nano-porosity and isolated, small crystallites of cristobalite and 3C-SiC. For the materials prepared at 1600°C , including the nano-composites, the continuous matrix phase is a silica phase. It seems therefore appropriate to interpret the thermal conductivity of all the materials in terms of the conductivity of a continuous phase containing a low volume fraction of isolated particles. This can be modeled in terms of the Maxwell model of thermal conductivity.¹⁹ In this model, the thermal conductivity of the material, κ^* , is only weakly dependent on the conductivity, κ_p , of isolated second phase and its volume fraction, f . For randomly oriented, spherical particles with no interfacial thermal resistance, the model conductivity reduces to:

$$\kappa^*/\kappa_m = 1 + \frac{f}{(1-f)/3 + [\kappa_m/(\kappa_p - \kappa_m)]} \quad (3)$$

where κ_m is the thermal conductivity of the continuous, matrix phase where there is no interfacial thermal resistance.²⁰

The results raise several questions, including what the thermal conductivity of the pure Si–O–C glass phases are and the possible origin of the variations with composition in the high-temperature plateau value of the thermal conductivity, from about 0.75 to $2.0\text{ W}\cdot(\text{m}\cdot\text{K})^{-1}$. While these variations would not be considered large in measurements of crystalline materials, they are significant for materials that already have low conductivity. Because all the materials studied, as evidenced by the microscopy observations and Raman spectra contain excess carbon, and the thermal conductivity is a second-order tensor averaged over the entire sample volume, the answers to these questions depend not only on the form and volume fraction but also on the spatial distribution of the carbon. All the samples were highly resistive, electrically, indicating that the carbon phase was not percolating, consistent with the microscopy observations.

The fraction of excess carbon can be readily estimated although some loss occurs during processing. According to the chemical formula of these Si–O–C materials, denoted as SiO_xC_y , they should consist of a glass with a molar fraction of $(x/2)\text{ SiO}_2 + (1-x/2)\text{ SiC}$ together with a carbon fraction given by $[(y-1-x/2)\text{ C}]$. (The ideal network glass can have a range of composition but would lie along the $\text{SiO}_2 - \text{SiC}$ tie line without any excess carbon, corresponding to a SiO_xC_y formula with $y = 1 - x/2$). At higher processing temperatures, such as after hot-pressing at 1600°C , the amorphous phase partitions into a SiO_2 matrix with the formation of SiC and possibly some mass loss of carbon due to the competing carbothermal decomposition of silica. As indicated in table I, the volume fraction of “free” carbon is calculated to be between 5% and 15%. The thermal properties of a variety of forms of carbon, including diamond, graphene, graphite, and amorphous carbons have recently been reviewed by Balandin et al.²¹ From the compiled data, it is evident that all forms of carbon other than amorphous carbon and pyrolytic graphite perpendicular to the planes¹⁶ have conductivities above room temperature significantly greater than that of the materials we have examined. So, even if graphitic carbon or graphene exists in these materials, as has been postulated,²² its effect on thermal conductivity is unlikely to be significant unless it forms a continuous network. This is considered unlikely as no electrical conductivity was

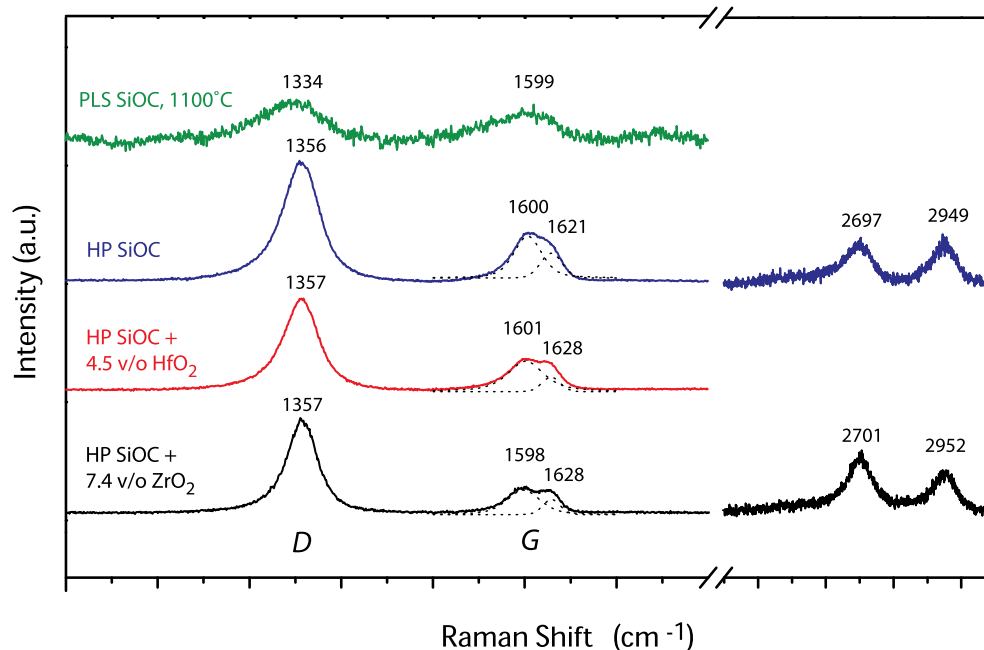


Fig. 3. Raman spectra from the sintered base Si–O–C material (top) and the hot-pressed materials whose thermal conductivities are reported in Fig. 2. The lines labeled D and G are the lines reported for sp^3 coordinated diamond and sp^2 coordinated graphite and graphene. Where spectra in the range 2700–3000 cm^{-1} are not shown, they were too weak to distinguish peaks. (For clarity of presentation, the Raman spectra are off-set vertically from one another).

measured. In addition, there remains considerable uncertainty in the thermal conductivity of amorphous carbon. Bullen et al.¹⁴ have convincingly shown that the thermal conductivity of amorphous carbons correlates with their density and Shamsa et al.¹⁵ have shown that the conductivity of diamond-like carbon films also depends on their thickness. Similarly, it is of interest to compare our results with those of amorphized SiC. Amorphous SiC does not occur in nature, but can be formed by either neutron irradiation, above a critical dose, or by sputtering. The former has a lower density than that of crystalline SiC²³ and material prepared by the latter not only has a lower density but is believed to be stabilized by hydrogen introduced during sputter deposition. Although the data is limited, there is a strong dependence of the measured thermal conductivity on the SiC density as is also found for amorphous carbon.¹⁴ Nevertheless, the lowest thermal conductivity reported for any form of amorphous SiC is $\sim 4 \text{ W}\cdot(\text{m}\cdot\text{K})^{-1}$ at room temperature, is still substantially greater than the conductivities we measure for the silicon oxycarbide glasses or reported for fused silica. Also, it is important to note that the two hot-pressed materials in Figs. 1 and 2 both have higher thermal conductivities than that of the 1100°C material and these two are predominately amorphous silica. So, taken together, these considerations suggest that the thermal conductivity of the pure Si–O–C network compound can be expected to be larger than that of fused silica. Clearly, refinements in making the Si–O–C amorphous phase without excess carbon are needed in order to make direct measurements of the thermal conductivity and for comparison with models of the thermal conductivity.

Turning to the variability in the values of thermal conductivity, there are several possibilities. The first is that there is a systematic variation in thermal conductivity with the O/C ratio along the SiO_2 –SiC tie line. A second is that some of this variability may be due to the presence of varying volume fractions of isolated second phases, such as β -SiC and ZrO_2 . However, as implied above, the largest uncertainty is probably associated with the contribution to the overall thermal conductivity of the carbonaceous phase, its volume fraction and its microstructural continuity. The Raman spectra indicate that all the materials contain both sp^3 - and sp^2 -bonded

carbon but doesn't inform about their spatial distributions. Electron microscopy observations of the same materials reveal that carbon occurs in a variety of microstructural forms. Some observations indicate small inclusions of carbon whereas others indicate that turbostratic carbon coats dispersed particles. There are also observations suggesting that there are carbon strands or sheets that decorate what appear to be the remnant interfaces formed between the precursor polymer particles as the materials densified.²⁴ At this stage, without three-dimensional tomographic imaging, we cannot determine the spatial distribution of carbon and whether it forms local percolating conducting paths in places through the materials.

An additional variability comes from the fact that the composition of the final materials cannot presently be closely controlled even when starting with the identical amounts of the precursor polymers. Consequently, there is some compositional variability that, in turn, can affect overall thermal conductivity values. For instance, an almost identical thermal conductivity is exhibited by the two hot-pressed materials, despite their different O and C contents. (All the compositions listed are those determined postfabrication). Some of the variability is probably due to differences in the loss of CO vapor from the surfaces of the polymer precursor particles that can occur during the densification of these particles while there remains open porosity for its escape from the material until all of the porosity closes.

The fact that the thermal conductivity of the $\text{SiO}_{1.59}\text{C}_{0.66}$ material hot-pressed at 1600°C is almost identical to that reported for fused silica is probably coincidental since it also contains free carbon. However, observations by TEM of the materials, as well as the composites containing zirconia and hafnia,⁴ indicate that they consists of a continuous matrix of silica and isolated, dispersed particles of β -SiC. Since the silica is the percolating, matrix phase it is not surprising that the conductivity is similar to that of fused silica.

In summary, we report that the thermal conductivities of several amorphous silicon oxycarbide compounds are similar to that of fused silica and exhibit almost temperature-independent thermal conductivities between about 200°C and 1000°C with small variations dependent on their precise

composition and the maximum temperature they were subjected to. Based on the values of their thermal conductivities as well as the temperature independence above room temperature, these amorphous materials can be considered to consist of a continuous network structure containing a secondary carbon phase that, depending on heat treatment, can be either spatially isolated carbon clusters or a percolating carbon phase, possibly graphitic or turbostratic carbon. From a practical materials selection perspective, this work suggests that, at least up to use temperatures of 1600°C, the thermal conductivity will not exceed a value of $2 \text{ W} \cdot (\text{m} \cdot \text{K})^{-1}$ even with 6–10 vol% of nanometer-sized hafnia or zirconia dispersoids. At still higher temperatures, when the carbothermal decomposition is complete with the conversion of the carbon to crystalline SiC, it is likely that the thermal conductivity will increase.

Acknowledgments

The authors are grateful to the Office of Naval Research under grant N00014-012-1-0993 for support of the research performed at Harvard and to the Humboldt Foundation for a Feodor Lynen Fellowship for AG at Harvard. We are also grateful to the Netzsch Instruments for making the thermal diffusivity measurements below room temperature.

References

- ¹A. Saha and R. Raj, "Crystallization Maps for SiCO Amorphous Ceramics," *J. Am. Ceram. Soc.*, **90** [2] 578–83 (2007).
- ²P. Colombo, R. Riedel, G. D. Soraru and H. J. Kleebe eds. *Polymer Derived Ceramics: From Nano-Structures to Applications*, 476. DEStech Publications, Inc., Lancaster, Pennsylvania, 2010.
- ³H. Zhang and C. G. Pantano, "Synthesis and Characterization of Silicon Oxycarbide Glasses," *J. Am. Ceram. Soc.*, **73**, 958–63 (1990).
- ⁴E. Ionescu, et al., "Polymer-Derived SiOC/ZrO₂ Ceramic Nanocomposites with Excellent High-Temperature Stability," *J. Am. Ceram. Soc.*, **93** [1] 241–50 (2010).
- ⁵S. Brahmandam and R. Raj, "Novel Composites Constituted from Hafnia and a Polymer-Derived Ceramic as an Interface: Phase for Severe Ultrahigh Temperature Applications," *J. Am. Ceram. Soc.*, **90** [10] 3171–6 (2007).
- ⁶P. Colombo, et al., "Polymer-Derived Ceramics: 40 Years of Research and Innovation in Advanced Ceramics," *J. Am. Ceram. Soc.*, **93** [9] 1805–37 (2010).
- ⁷C. Kittel, "Interpretation of the Thermal Conductivity of Glasses," *Phys. Rev.*, **75** [6] 972–4 (1949).
- ⁸G. A. Slack, "Solid State Physics-Advances in Research and Applications,"; pp. 1–9, Vol 34, Edited by F. Seitz and A. G. Turnbull. Academic Press, New York, NY, 1979.
- ⁹D. G. Cahill and R. O. Pohl, "Heat-Flow and Lattice-Vibrations in Glasses," *Solid State Commun.*, **70** [10] 927–30 (1989).
- ¹⁰G. Grimvall, *Thermophysical Properties of Materials*. North Holland, Amsterdam, 1986.
- ¹¹K. W. Schlichting, N. P. Padture, and P. G. Klemens, "Thermal Conductivity of Dense and Porous Ytria-Stabilized Zirconia," *J. Mater. Sci.*, **36** [12] 3003–10 (2001).
- ¹²B. Papendorf, et al., "High-Temperature Creep Behavior of Dense SiOC-Based Ceramic Nanocomposites: Microstructural and Phase Composition Effects," *J. Am. Ceram. Soc.*, **96** [1] 272–80 (2013).
- ¹³H. J. Kleebe, et al., "Evolution of C-Rich SiOC Ceramics," *Int. J. Mater. Res.*, **97** [6] 699–709 (2006).
- ¹⁴A. J. Bullen, et al., "Thermal Conductivity of Amorphous Carbon Thin Films," *J. Appl. Phys.*, **88** [11], 6317–20 (2000).
- ¹⁵M. Shamsa, et al., "Thermal Conductivity of Diamond-Like Carbon Films," *Appl. Phys. Lett.*, **89**, 161921–3 (2006).
- ¹⁶G. A. Slack, "Anisotropic Thermal Conductivity of Pyrolytic Graphite," *Phys. Rev.*, **127**, 694–701 (1962).
- ¹⁷D. S. Knight and W. B. White, "Characterization of Diamond Films by Raman Spectroscopy," *J. Mater. Res.*, **4** [2] 385–93 (1989).
- ¹⁸A. C. Ferrari and J. Robertson, "Interpretation of Raman Spectra of Disordered and Amorphous Carbon," *Phys. Rev. B*, **61** [20] 14095–107 (2000).
- ¹⁹W. D. Kingery, H. K. Bowen, and D. R. Uhlmann, *Introduction to Ceramics*. John Wiley, New York City, New York, 1960.
- ²⁰C.-W. Nan, R. Birringer, and D. R. Clarke, "Effective Thermal Conductivity of Particulate Composites with Interfacial Thermal Resistance," *J. Appl. Phys.*, **81** [10] 6692–9 (1997).
- ²¹A. A. Balandin, "Thermal Properties of Graphene and Nanostructured Carbon Materials," *Nat. Mater.*, **10**, 569–81 (2011).
- ²²A. Scarmi, G. D. Soraru, and R. Raj, "The Role of Carbon in the Unexpected Visco(an)Elastic Behavior of Amorphous Silicon Oxycarbide Above 1273 K," *J. Non-Cryst. Solids*, **351**, 2238–43 (2005).
- ²³L. L. Snead and S. J. Zinkle, "Structural Relaxation in Amorphous Silicon Carbide," *Nuclear Instr. Methods Phys. Res. B*, **191**, 497–503 (2002).
- ²⁴B. Papendorf, et al., "High-Temperature Creep Behavior of Dense SiOC-Based Ceramic Nanocomposites: Microstructural and Phase Composition Effects," *J. Am. Ceram. Soc.*, **96** [1], 272–80 (2013).
- ²⁵D. G. Cahill, Thermal Conductivity Data, <http://users.mrl.illinois.edu/cahill/tcdata/tcdata.html>, accessed on 14/09/2015, (2014).
- ²⁶C. Y. Ho, R. W. Powell, and P. E. Liley, "Thermal Conductivity of the Elements," *J. Phys. Chem. Ref. Data*, **3** [Suppl. 1], 1–796 (1974). □